Gravitational Microlensing Events in the Optical Lightcurve of Active Galaxy S5 0716+714

D. Ł. Król, Ł. Stawarz, J. Krzesiński and C. C. Cheung

Source: 2MASS

Different regimes

Gravitational lensing

Strong lensing

Weak lensing

Mico-lensing

HE0435-1223, ESA/Hubble

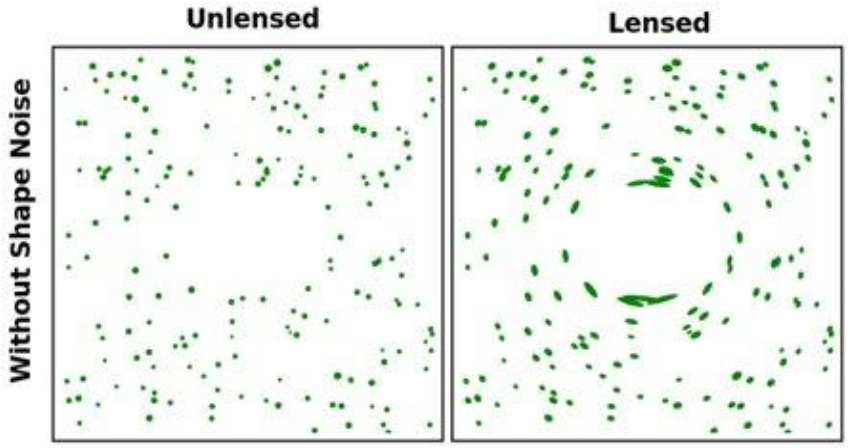

https://commons.wikimedia.org/wiki/File:Shapenoise.svg

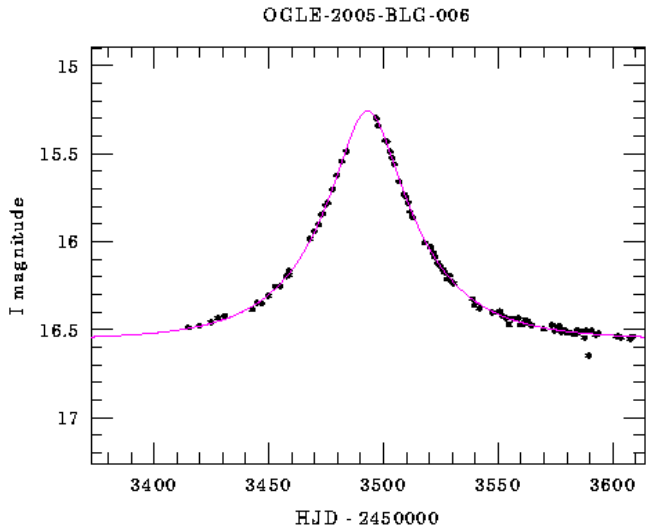

OGLE-2005-BLG-006, https://ogle.astrouw.edu.pl/ogle3/ews/2005/blg-006.html

Microlensing of Galactic sources

Ocures when multiple images are unresolved – we see only the change of the brightness of the source. Micro lensing is **achromatic**.

Microlensing allows detecting objects normally impossible to detect (e.g., exoplanets, Massive Compact Halo Objects).

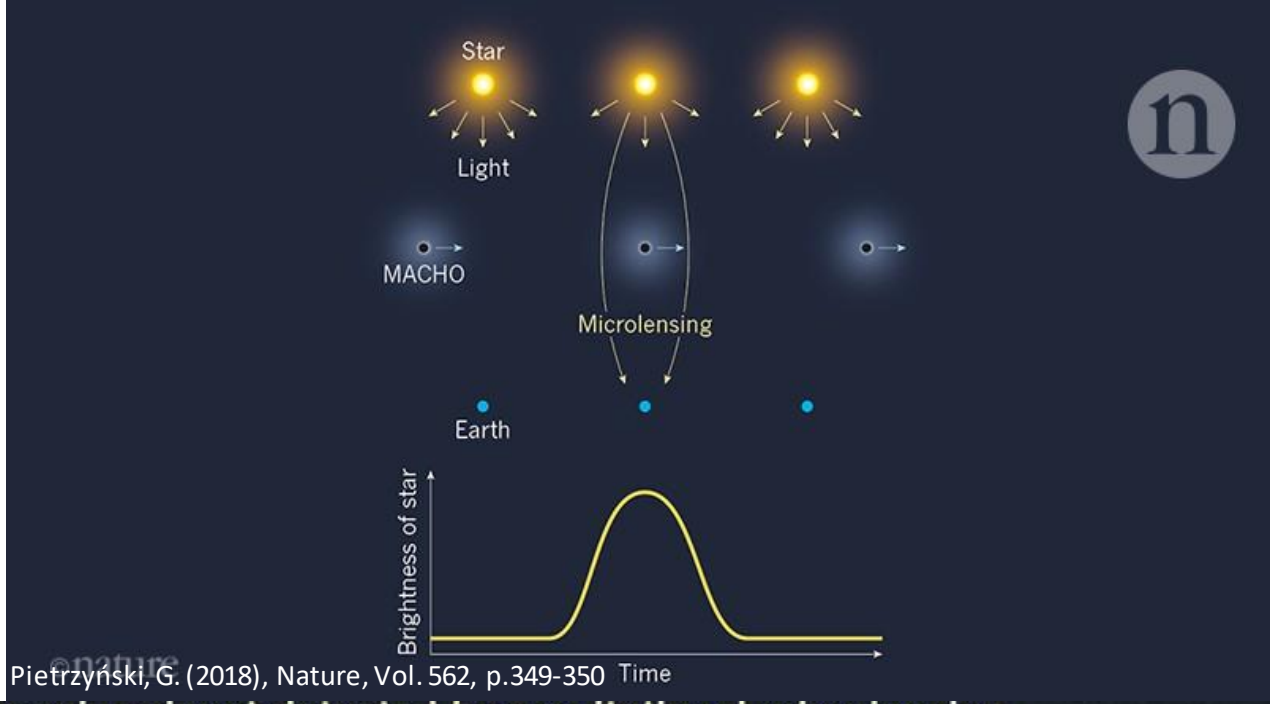

Pietrzyński, G. (2018), Nature, Vol. 562, p.349-350

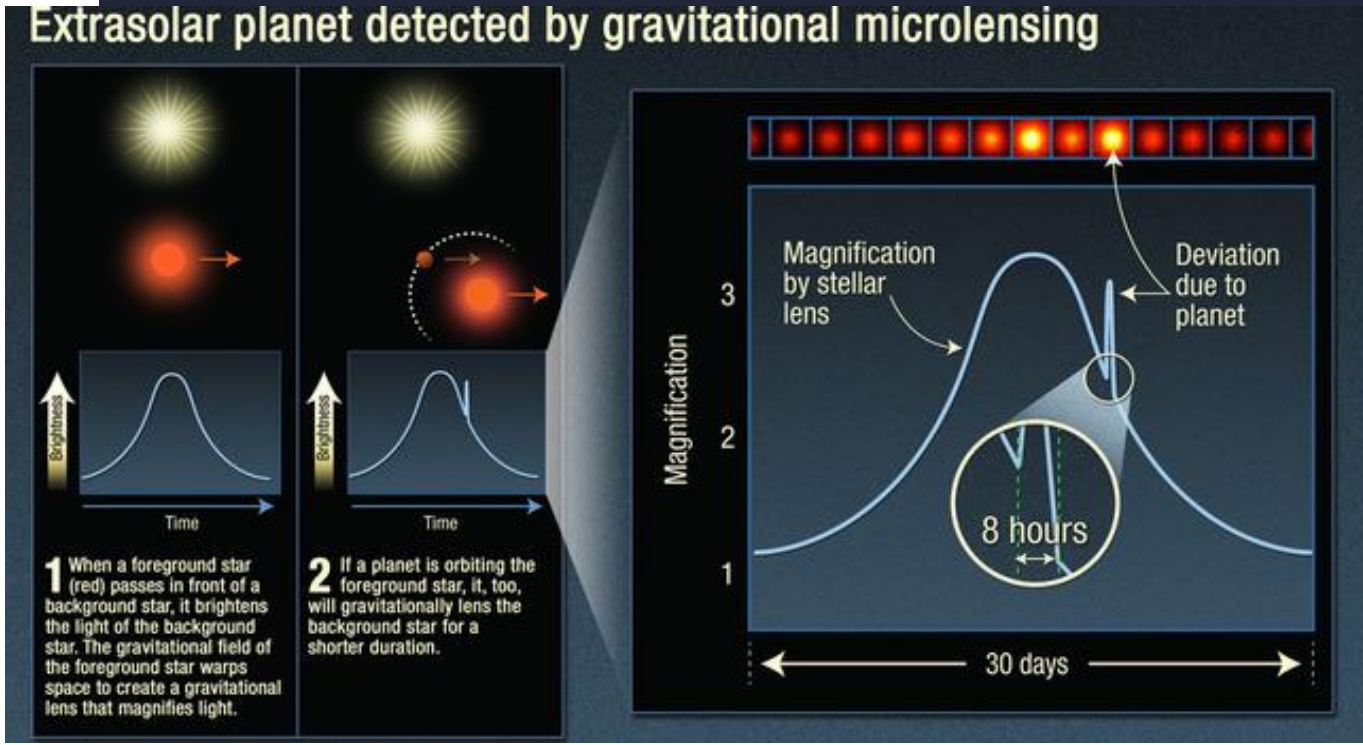

Image Credit: NASA / ESA / K. Sahu / STScI, https://www.universetoday.com/wp-content/uploads/2014/03/hs-2012-07-b-web_print.jpg

Binary lens

Mao & Paczyński 1991: we expect that most of the stellar objects are in binary systems

Depending on mass ratio and separation of binary magnification patterns may differ.

Magnification pattern

Source trajectories on the lens plane

Magnification curves

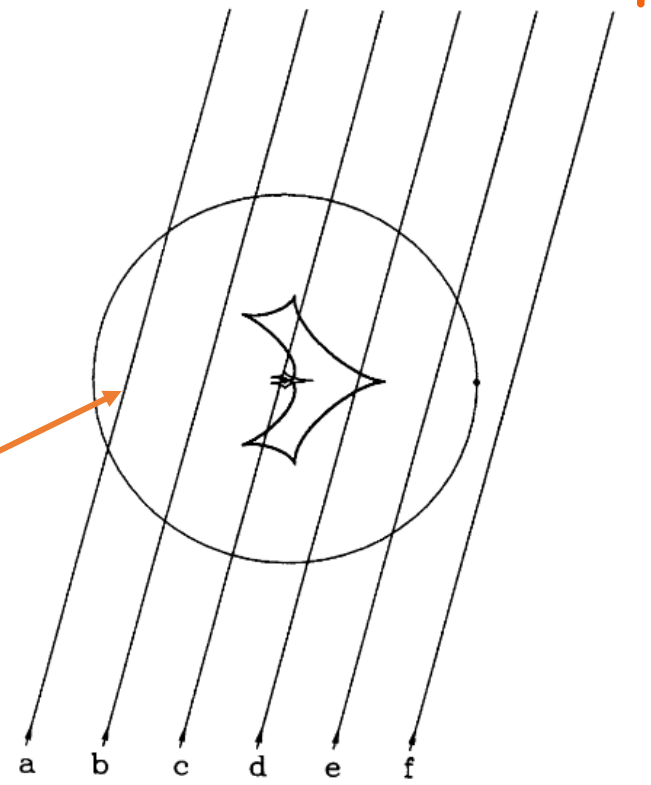

FIG. 1.—Geometry of microlensing by a binary, as seen in the sky. The primary star of 1 $M_\odot$ is located at the center of the figure, and the secondary of 0.1 $M_\odot$ or 0.001 $M_\odot$ is located on the right, on the Einstein ring of the primary. The radius of the ring is 1.0 mas for a source located at a distance of 8 kpc and the lens at 4 kpc. The two complicated shapes around the primary are the caustics: the larger and the smaller corresponding to the 0.1 $M_\odot$ and 0.001 $M_\odot$ companions, respectively. If a source is located outside these regions, then only three microimages are formed, while a source inside them forms five microimages. The parallel straight lines indicate the trajectories of sources for which the light variations are shown in Fig. 2.

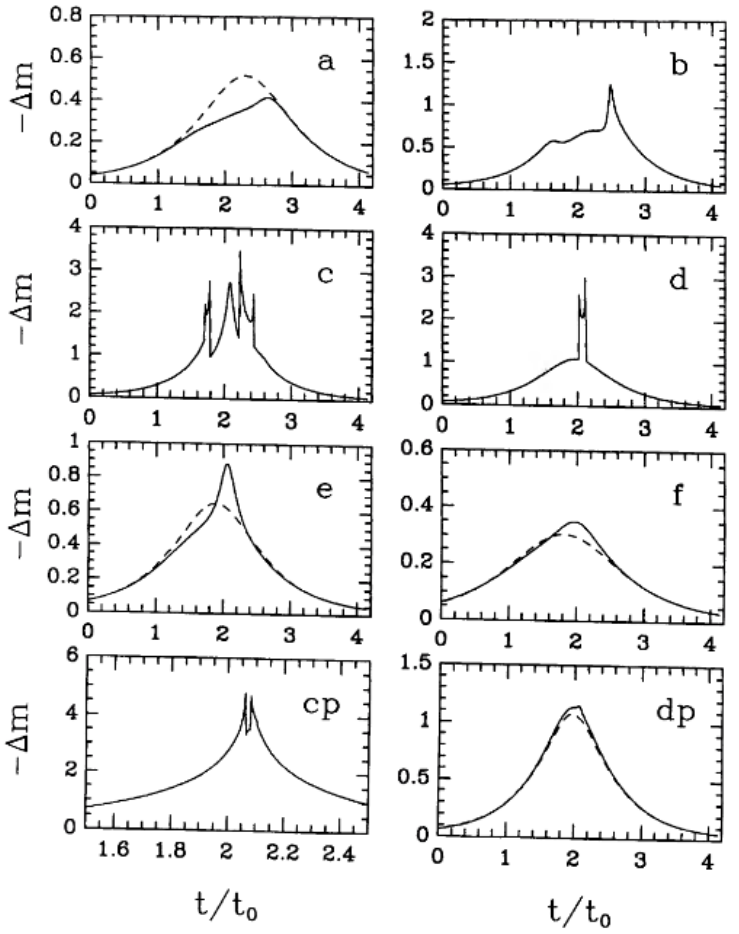

FIG. 2.—The light curves shown correspond to the six source trajectories in Fig. 1. The source is modeled as a uniform disk of radius $R_{star} = 10^{11}$ cm. The first six light curves, a–f, correspond to the case with a 0.1 $M_\odot$ companion; the last two, cp and dp, correspond to the case with a 0.001 $M_\odot$ companion. Notice very high spikes when a source crosses a caustic, or approaches a cusp, as in the light curves c, d, and cp. The low-amplitude light curves a, e, f, and dp,

Mao & Paczyński 1991

Idea: maybe gravitational lensing may explain at least part of AGN variability.

AGNs (especially blazars) are highly variable sources for a high range of frequencies and on different time scales ranging from hours to years.

The idea that microlensing may be responsible for part of the variability arose for the first time in the 80s.
Gopal-Krishna & Subramanian (1991) proposed that **achromatic optical variability of blazars on ~hours timescales may be due to gravitational microlensing of the relativistic jet knots.**

LETTERS TO NATURE

Gravitational micro-lensing of the relativistic jets of quasars

Gopal-Krishna & Kandaswamy Subramanian

Tata Institute of Fundamental Research, PO Bag No. 3, Poona University Campus, Pune 411007, India

GRAVITATIONAL microlensing of quasars has been invoked to account for their observed optical variability[1–3]—the timescale being as short as a few years for microlenses the size of Jupiter moving at ~300 km s^{-1} (ref. 4). But some blazars (conspicuously active quasars) show ultra-rapid variability on timescales as short as 1 hour in the optical[5–7] and 1 day at centimetre wavelengths[8–11]. Blazars are known to contain relativistic jets directed within ~10° of the line of sight[12], and bright knots in these jets could appear to move superluminally with respect not only to the blazar nucleus but also to any galaxy near the line of sight. We argue here that any such superluminal motion[13], if microlensed by a star in an intervening galaxy, can produce the requisite ultra-rapid variations, even in the absence of intrinsic flux variations in the jet. Moreover, the same mechanism can naturally account for the commonly observed ~1-day variability of compact radio sources at centimetre wavelengths[14].

XXIst century idea resurrection:

Symmetric Achromatic Variability in Active Galaxies: A Powerful New Gravitational Lensing Probe?

H. K. Vedantham[1], A. C. S. Readhead[1], T. Hovatta[2,3,4], T. J. Pearson[1], R. D. Blandford[5], M. A. Gurwell[6], A. Lähteenmäki[2], W. Max-Moerbeck[7], V. Pavlidou[8], V. Ravi[1], R. A. Reeves[9], J. L. Richards[1], M. Tornikoski[2], and J. A. Zensus[7]

[1] Owens Valley Radio Observatory, California Institute of Technology, Pasadena, CA 91125, USA
[2] Aalto University Metsähovi Radio Observatory, Metsähovintie 114, FI-02540 Kylmälä, Finland
[3] Aalto University Department of Radio Science and Engineering, Finland
[4] Tuorla Observatory, Department of Physics and Astronomy, University of Turku, Finland
[5] Kavli Institute for Particle Astrophysics and Cosmology, Department of Physics, and SLAC National Accelerator Laboratory, Stanford University, Stanford, CA 94305, USA
[6] Harvard-Smithsonian Center for Astrophysics, Cambridge, MA 02138, USA
[7] Max-Planck-Institut für Radioastronomie, Auf dem Hügel 69, D-53121 Bonn, Germany
[8] Department of Physics and Institute of Theoretical and Computational Physics, University of Crete, 71003 Heraklion, Greece and Foundation for Research and Technology—Hellas, IESL, 7110 Heraklion, Greece
[9] CePIA, Astronomy Department, Universidad de Concepción, Casilla 160-C, Concepción, Chile

Received 2017 February 8; revised 2017 May 2; accepted 2017 May 16; published 2017 August 15

Selection of the lensing candidates from the radio monitoring programs (OVRO 15 GHz, Metsähovi 22 and 37 GHz, OVRO 100 GHz, SMA 234 GHz).

The most promising candidate: J1415+1320.

Shows four one-year long U-shaped Symmetric Achromatic Variability (SAV) events.

Symmetric Achromatic Variability in Active Galaxies: A Powerful New Gravitational Lensing Probe?

H. K. Vedantham[1], A. C. S. Readhead[1], T. Hovatta[2,3,4], T. J. Pearson[1], R. D. Blandford[5], M. A. Gurwell[6], A. Lähteenmäki[2], W. Max-Moerbeck[7], V. Pavlidou[8], V. Ravi[1], R. A. Reeves[9], J. L. Richards[1], M. Tornikoski[2], and J. A. Zensus[7]
[1] Owens Valley Radio Observatory, California Institute of Technology, Pasadena, CA 91125, USA
[2] Aalto University Metsähovi Radio Observatory, Metsähovintie 114, FI-02540 Kylmälä, Finland
[3] Aalto University Department of Radio Science and Engineering, Finland
[4] Tuorla Observatory, Department of Physics and Astronomy, University of Turku, Finland
[5] Kavli Institute for Particle Astrophysics and Cosmology, Department of Physics, and SLAC National Accelerator Laboratory, Stanford University, Stanford, CA 94305, USA
[6] Harvard-Smithsonian Center for Astrophysics, Cambridge, MA 02138, USA
[7] Max-Planck-Institut für Radioastronomie, Auf dem Hügel 69, D-53121 Bonn, Germany
[8] Department of Physics and Institute of Theoretical and Computational Physics, University of Crete, 71003 Heraklion, Greece and Foundation for Research and Technology—Hellas, IESL, 7110 Heraklion, Greece
[9] CePIA, Astronomy Department, Universidad de Concepción, Casilla 160-C, Concepción, Chile
Received 2017 February 8; revised 2017 May 2; accepted 2017 May 16; published 2017 August 15

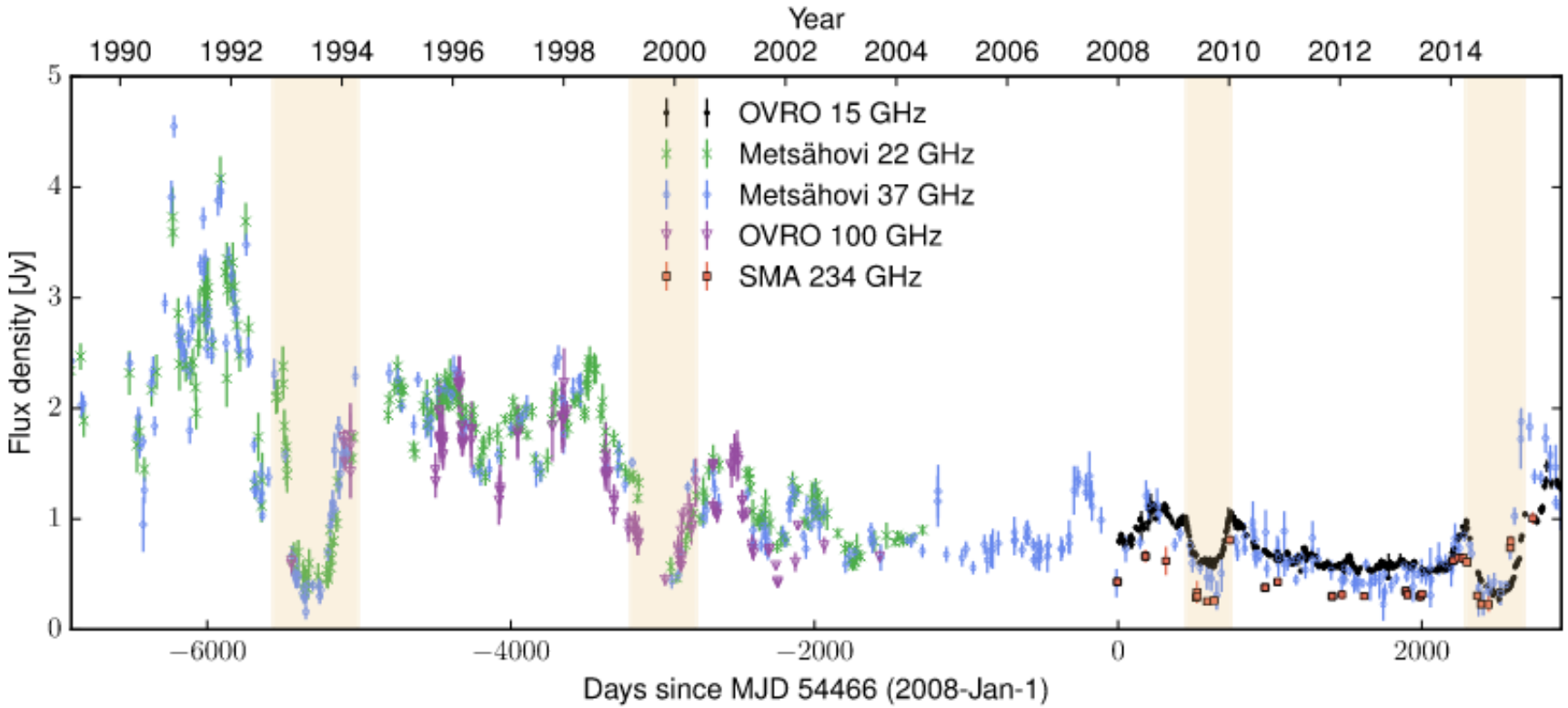

Figure 2. Same as Figure 1 but with the entire Metsähovi monitoring data at 22 and 37 GHz since 1989, and the OVRO MMA data at 100 GHz. Two more achromatic U-shaped events are seen in 1993 and 2000.

Vedantham et al. 2019

Fits in different frequencies

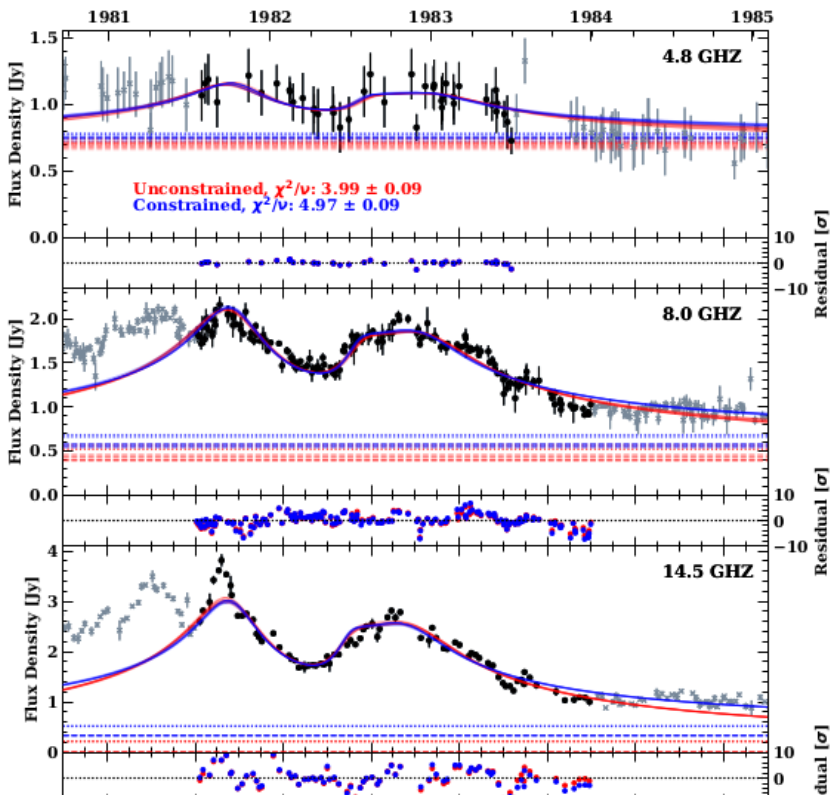

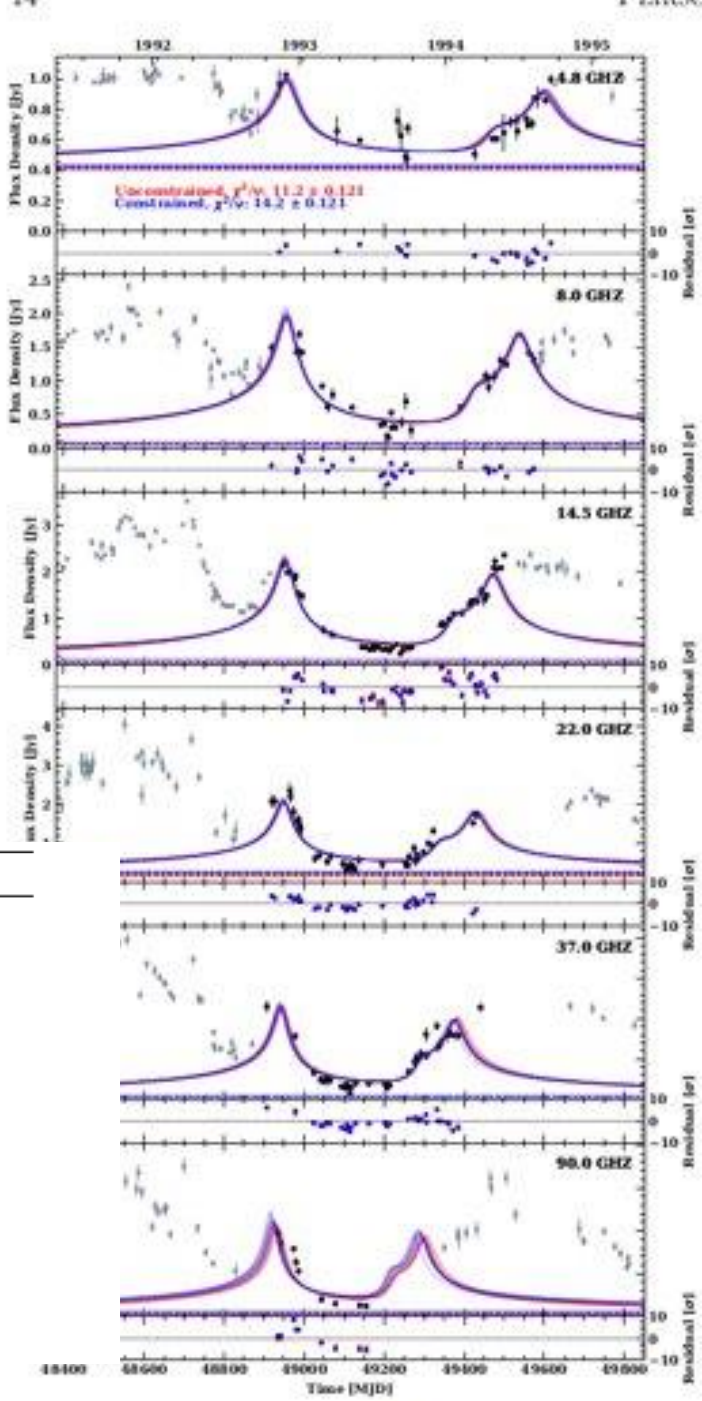

	SAV1	SAV2	SAV3	SAV4	SAV5
t_0 [MJD]	$45112.494^{+43.143}_{-70.513}$	$49298.693^{+87.800}_{-153.205}$	$51785.8411^{+77.9544}_{-202.4781}$	$55096.679^{+49.589}_{-79.878}$	$57029.745^{+84.722}_{-137.009}$
δu_0 [θ_E]	$-0.026^{+0.004}_{-0.004}$	$0.008^{+0.001}_{-0.001}$	$-0.047^{+0.0585}_{-0.0184}$	$-0.028^{+0.051}_{-0.030}$	$0.007^{+0.002}_{-0.002}$
t_E [days]	$3377.133^{+166.034}_{-230.442}$	$6535.783^{+64.019}_{-334.842}$	$6551.6575^{+48.2343}_{-305.3139}$	$3267.599^{+208.333}_{-264.855}$	$4936.219^{+207.969}_{-492.406}$
s	–	–	$1.1641^{+0.0324}_{-0.0186}$	$1.174^{+0.029}_{-0.020}$	–
q	–	–	$0.0087^{+0.0013}_{-0.0013}$	$0.006^{+0.001}_{-0.001}$	–
$\delta\alpha$[°]	$-5.006^{+1.110}_{-1.120}$	$-1.519^{+0.754}_{-0.851}$	$1.471^{+1.2125}_{-1.2833}$	$296.644^{+0.889}_{-0.945}$	$3.709^{+0.850}_{-0.931}$
k	–	–	$0.0188^{+0.0543}_{-0.0162}$	$0.046^{+0.047}_{-0.029}$	–
γ	–	–	$0.0327^{+0.0026}_{-0.0019}$	$0.026^{+0.002}_{-0.001}$	–
ϕ [rad]	–	–	$2.4303^{+0.0489}_{-0.0577}$	$2.495^{+0.036}_{-0.042}$	–

Microlensing Events in the Optical Lightcurve of Active Galaxy S5 0716+714

Microlensing Events in the Optical Lightcurve of Active Galaxy S50716+714

Blazar S5 0716+714:

- **Particularly high duty cycle** on short time scales at optical frequencies.
- Subject of numerous intra-night monitoring programs, e.g. Whole Earth Blazar Telescope (**WEBT**) and Transiting Exoplanet Survey Satellite (**TESS**).

Unprecedented data coverage of the light-curve on intra-night scale

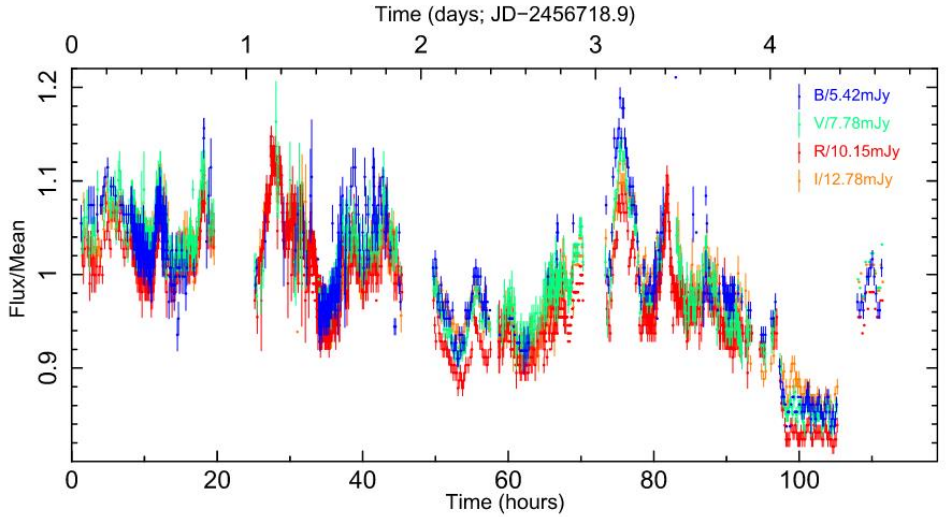

Figure 3. Mean-normalized photometric light curves of S5 0716+714 in *BVRI* filters (see the upper panels in Figure 1) facilitating a visual comparison of variability across the four bands.

Bhatta et al. 2016

Whole Earth Blazar Telescope (WEBT) Collaboration

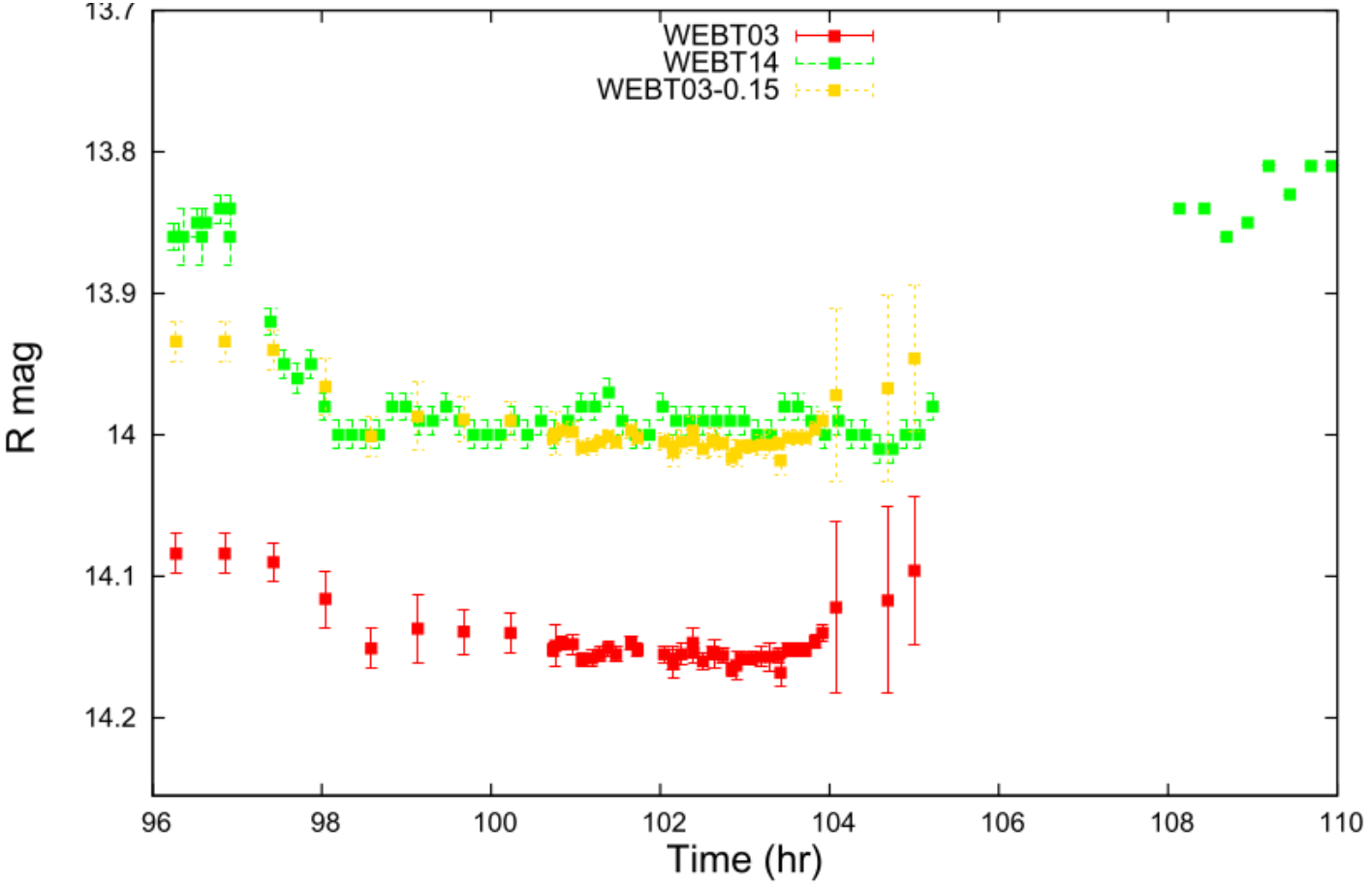

Bhatta et al. 2016

Peculiar achromatic "double-horn" maximum feature with the plateau in between was noted for the first time in Bhatta et al. 2016 ("*for about 6hr (…) the source suddenly exhibited a strongly reduced level of flux variability, resulting in a plateau in all four bands' light curves").*

Ostorero et al.2006
Bhatta et al. 2016

Similar events can be spotted in TESS data.

Inspired by the work (Vedantham et al. 2017) we propose that the we propose that the U-shaped features we see in the optical light curve of S5 0716+714, may as well result from the lensing of a precessing jet in the source by a binary lens.

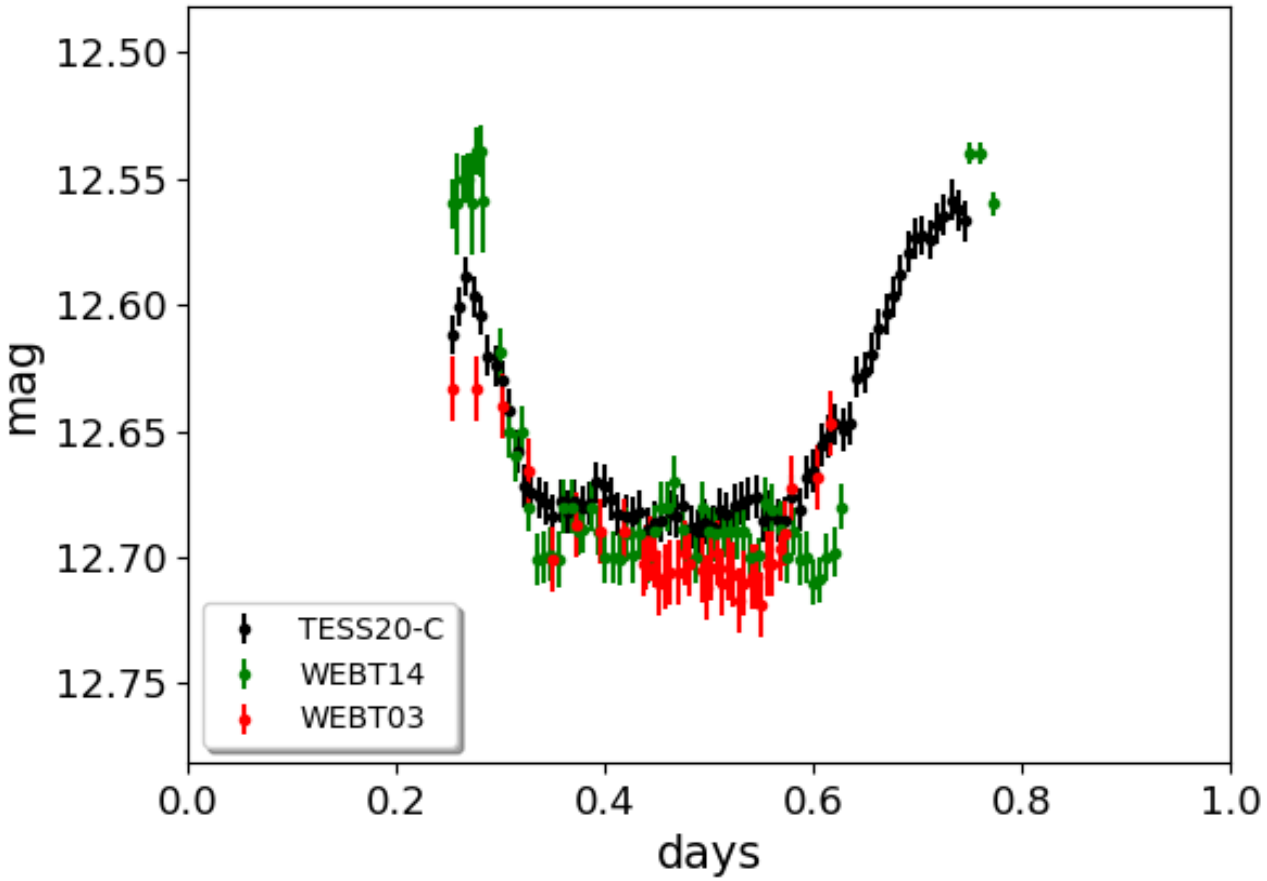

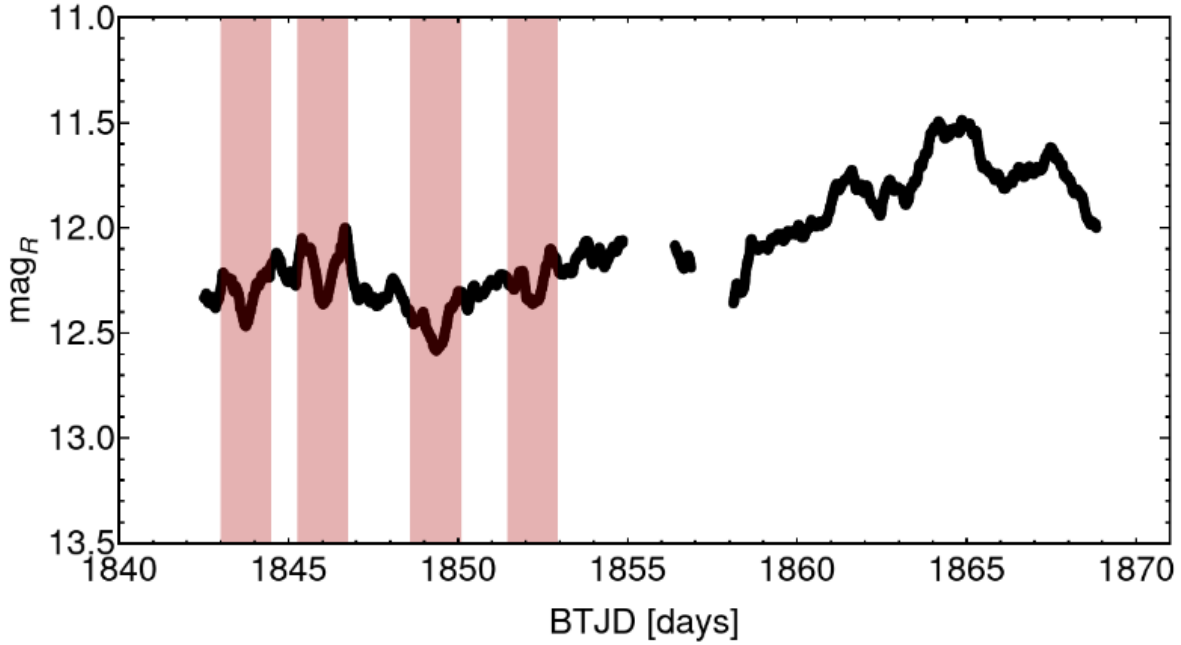

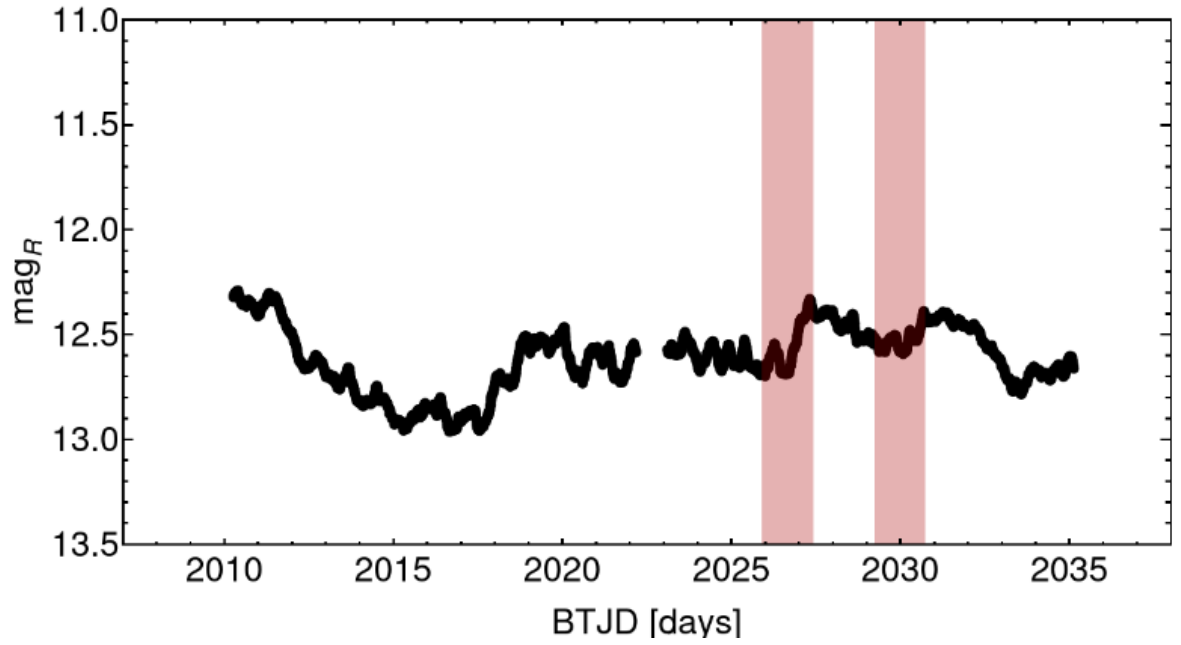

Achromacity

Four out of the six events, have the accompanying WEBT data (Raiteri et al. 2021) , which clearly show that the flux changes traced by the dense TESS sampling, are followed closely in all the B, V, R, and I filters separately

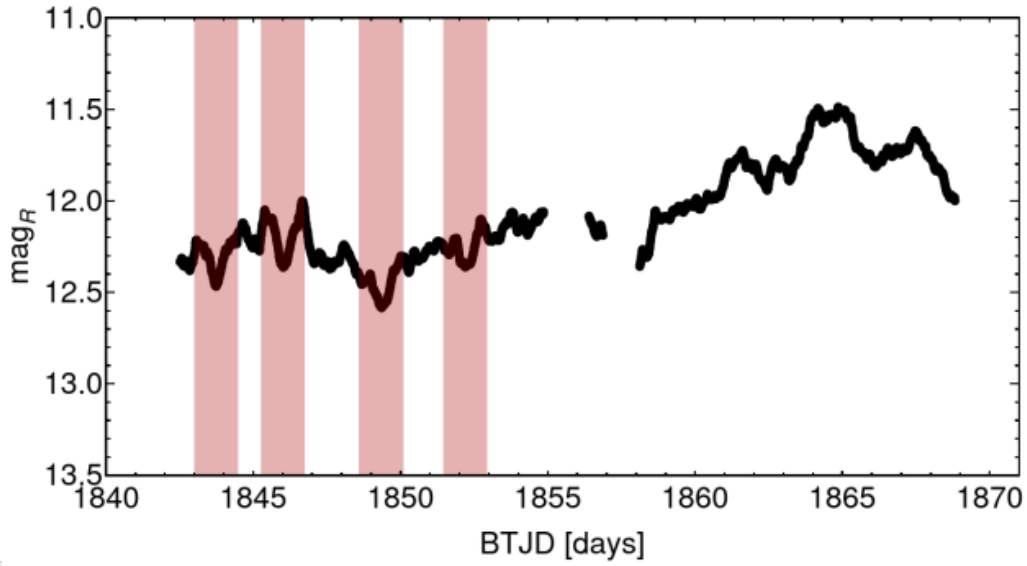

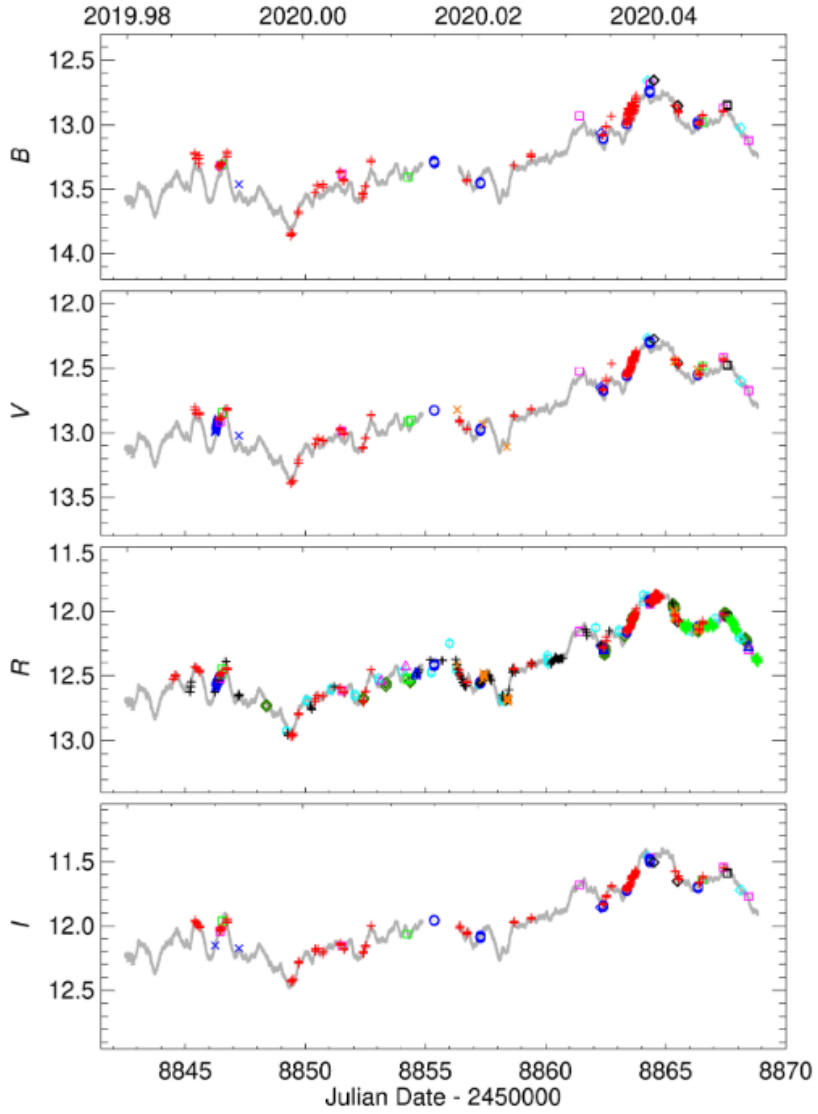

Figure 3. Light curves of S5 0716+714 in *BVRI* built with data from the WEBT Collaboration. Different symbols and colours distinguish different data sets as explained in Table 1. In all panels, the *TESS* light curve is plotted in grey, highlighting the excellent agreement between space- and ground-based data.

Raiteri et al. 2021

All the TESS events are possible to fit with the same binary lens model. It is also possible to fit WEBT events with this lens

It was difficult to find (q,d) for which it was possible to fit first two (TESS19-A andTESS19-B the rest of the events). On the other hand lot of trajectory parameters give similar fit quality.

Table 1. MULENSMODEL best-fit parameters.

Parameter	TESS19-A	TESS19-B	TESS20-A	TESS20-B	TESS20-C	TESS20-D
ρ	0.013^f	0.013^f	0.013^f	0.013^f	0.013^f	0.013^f
q	0.00545^f	0.00545^f	0.00545^f	0.00545^f	0.00545^f	0.00545^f
d	0.727^f	0.727^f	0.727^f	0.727^f	0.727^f	0.727^f
u_0	0.36	0.35	0.48	0.78	0.75	0.54
t_E	3.0	4.0	3.4	2.4	1.5	1.7
α	89	94	82	88	87	94
t_0 [BTJD]	1843.78	1845.92	1849.62	1852.30	2026.66	2030.00
t_0 [UTC]	2019-12-26	2019-12-28	2020-01-01	2020-01-03	2020-06-26	2020-06-29
	06:36	09:58	02:46	19:05	03:54	12:04
χ^2/dof	1.91	1.5	3.75	2.10	0.93	0.89

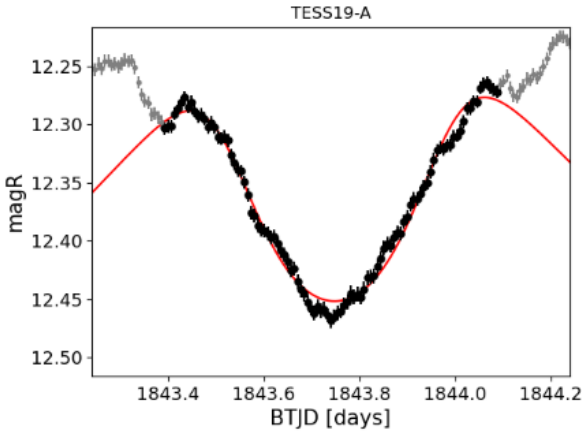

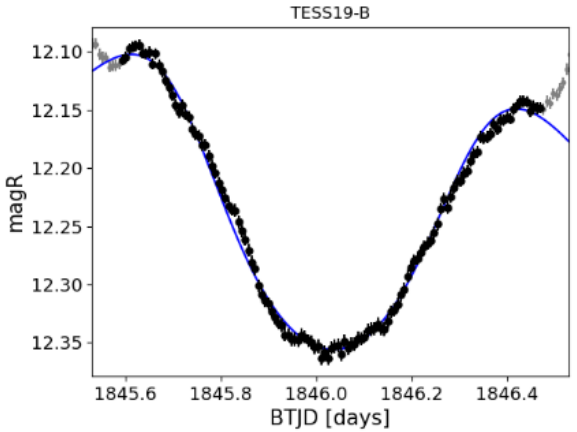

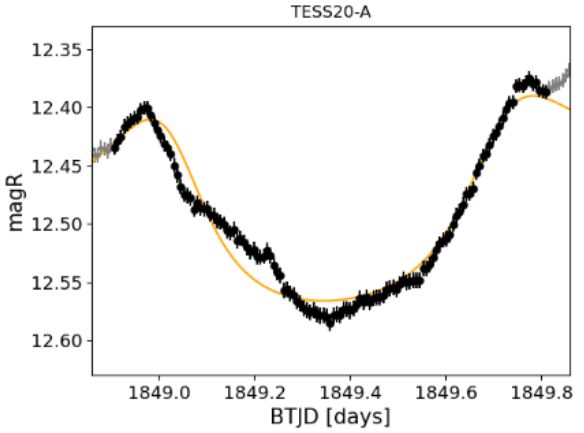

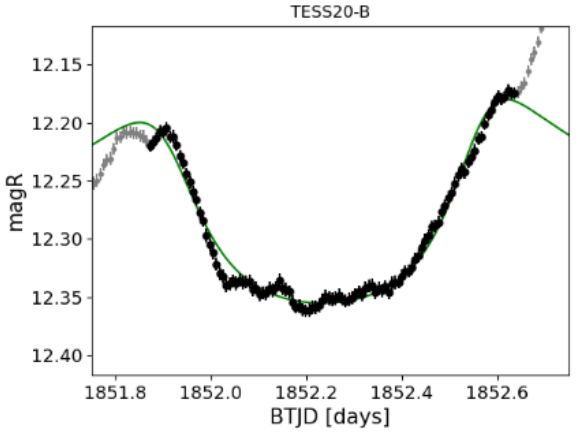

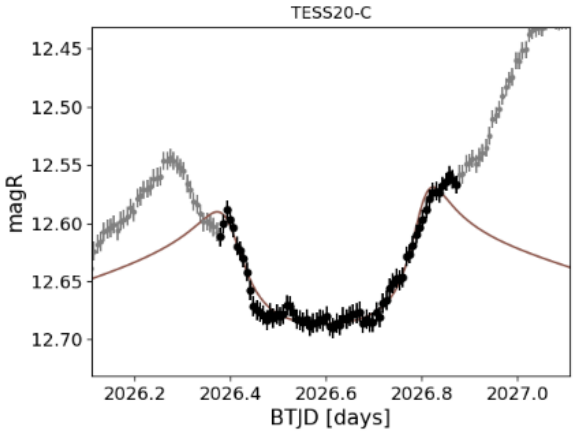

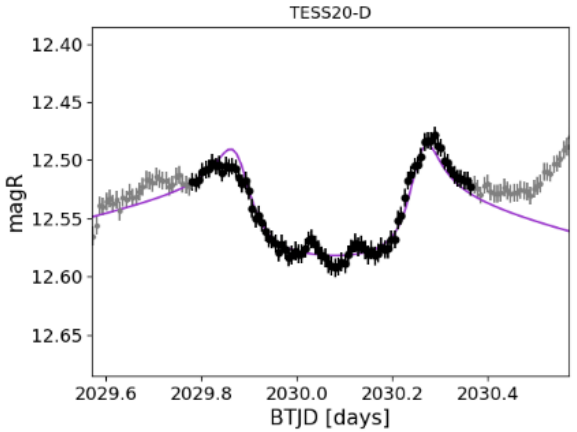

Lens binary system

- q=0.0054, d=0.7,
- q is the binary mass ratio,
- d is the binary separation in the Einstein radius units

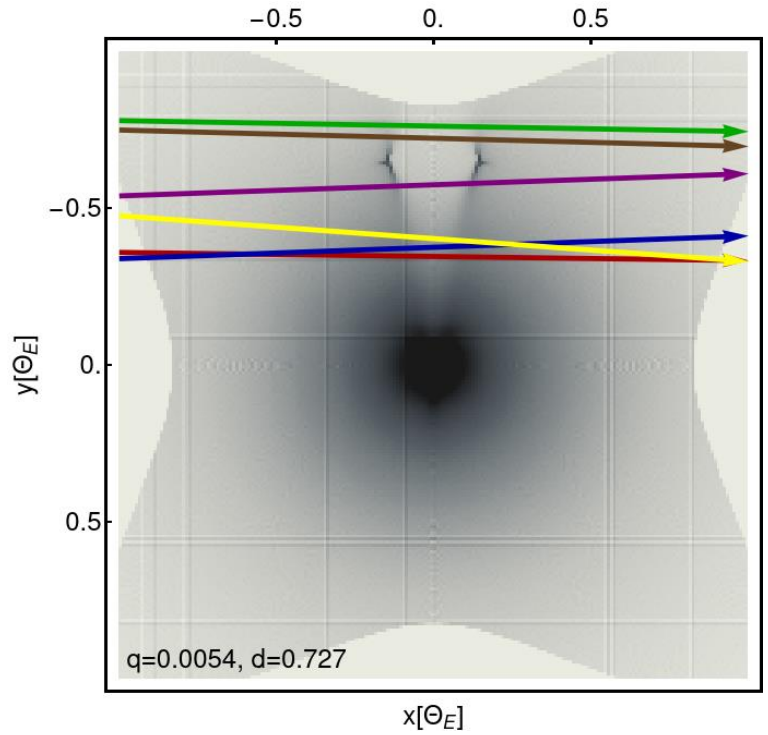

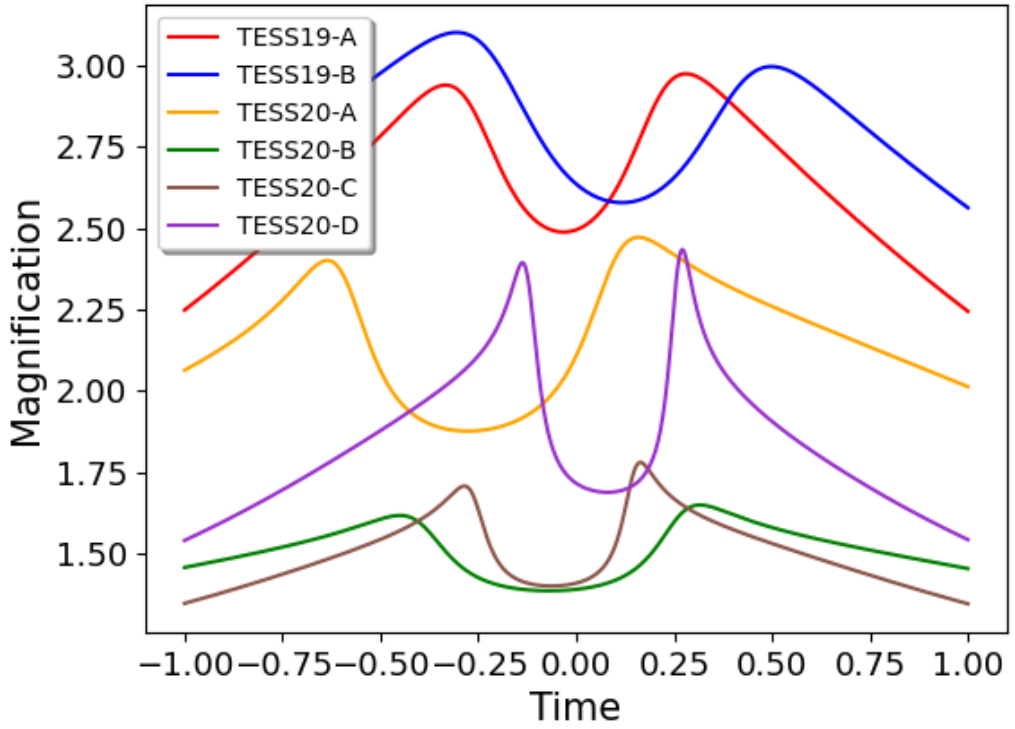

Constains on the lens mass

Size of the emission region in blazar cannot be smaller than gravitational radius of the SMBH in nucleus:

$$r_g = \frac{GM_\bullet}{c^2} \simeq \left(\frac{M_\bullet}{10^8 M_\odot}\right) \mathrm{AU}$$

Lens must be on the line of sight to the jet for at least ~20 years.

$$\sigma_{\mathrm{vel}}\,\tau < R_E$$

Assumption (based on modelling): $D_{LS} \ll D_L$, $D_S \approx D_L$

Lens is in the blazar host galaxy.

We can assume maximal apparent velocity (for this source 30). Then:

$$R_E = c\beta_{\mathrm{app}}\,t_E$$

Orbital period of the binnary has to be << than the time of the event.

$$v_{\mathrm{orb}}\,t_E \ll d\,R_E$$

$$\Theta_E = \left(\frac{4GM}{c^2}\,\frac{D_{\mathrm{LS}}}{D_{\mathrm{L}} D_{\mathrm{S}}}\right)^{1/2}$$

The binary lens mass

We know the time scale of the events from the fitting. Assuming maximal projected velocity βapp.

$$\left(\frac{M}{10^4\,M_\odot}\right) \simeq 10^4 \left(\frac{\beta_{\rm app}}{30}\right)^2 \left(\frac{t_E}{2\,{\rm d}}\right)^2 \left(\frac{D_{\rm LS}}{100\,{\rm pc}}\right)^{-1}$$

For a typical blazar with $M_\bullet \sim 10^8 M_\odot$, the velocity dispersion is expected to be around $\sigma_{\rm vel} \simeq 200$ km s^{-1} .

$$\left(\frac{M}{10^4\,M_\odot}\right) > 10^2 \left(\frac{\sigma_{\rm vel}}{200\,{\rm km/s}}\right)^2 \left(\frac{\tau}{20\,{\rm yr}}\right)^2 \left(\frac{D_{\rm LS}}{100\,{\rm pc}}\right)^{-1} \quad (2)$$

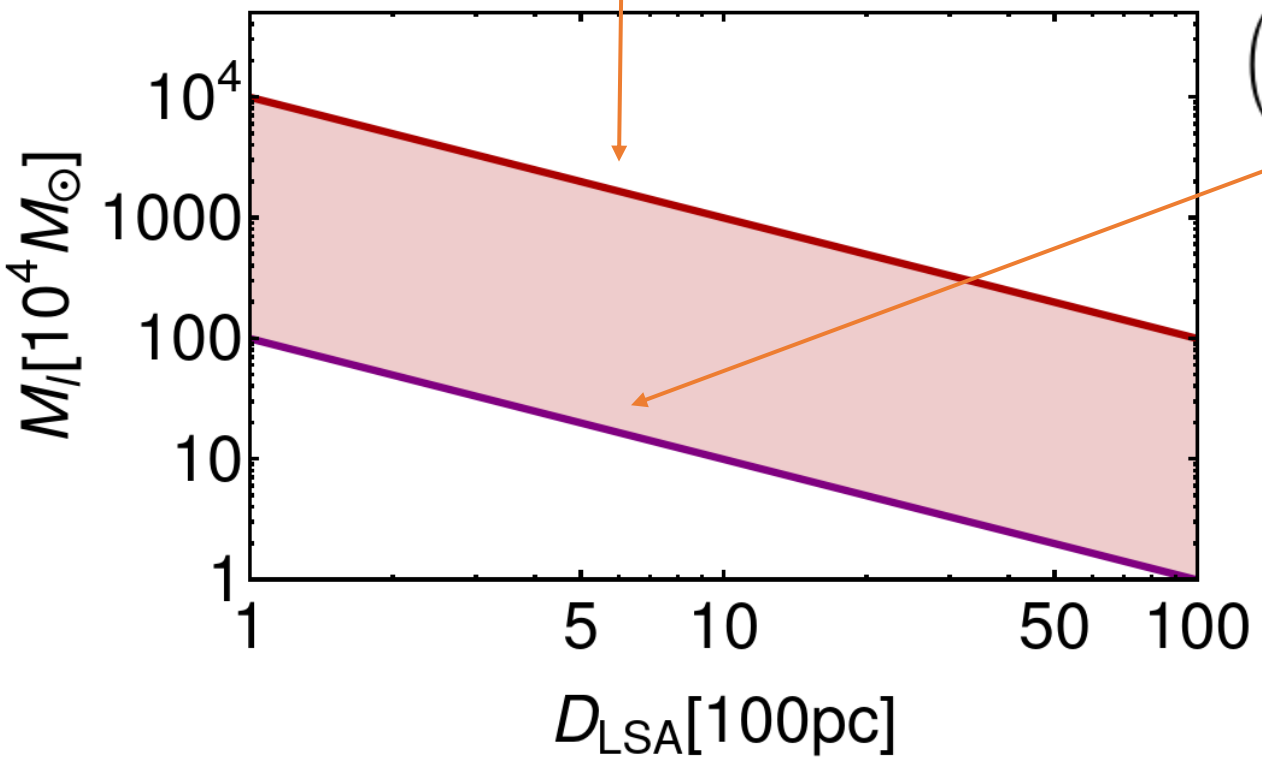

$10^6 < M/M_\odot < 10^8$ for the distance DLS ≃ 100 pc,
$10^4 < M/M_\odot < 10^6$ for $D_{LS} \simeq 10$ kpc.

What is our lens?

Mass consistent with the IMBH accompanied by the lower mass object.

The IMBH lens should be accompanied by a much less massive (ratio 1:200) object. N-body simulations of globular clusters show that we may expect IMBH with companions for these mass ranges (see, e.g., Konstantinidis et al. 2013, Leigh et al. 2013)

Laser Interferometer Space Antenna (LISA) is expected to detect ~2 mergers of BHs in this mass range per year (Amaro-Seoane et al.2022).

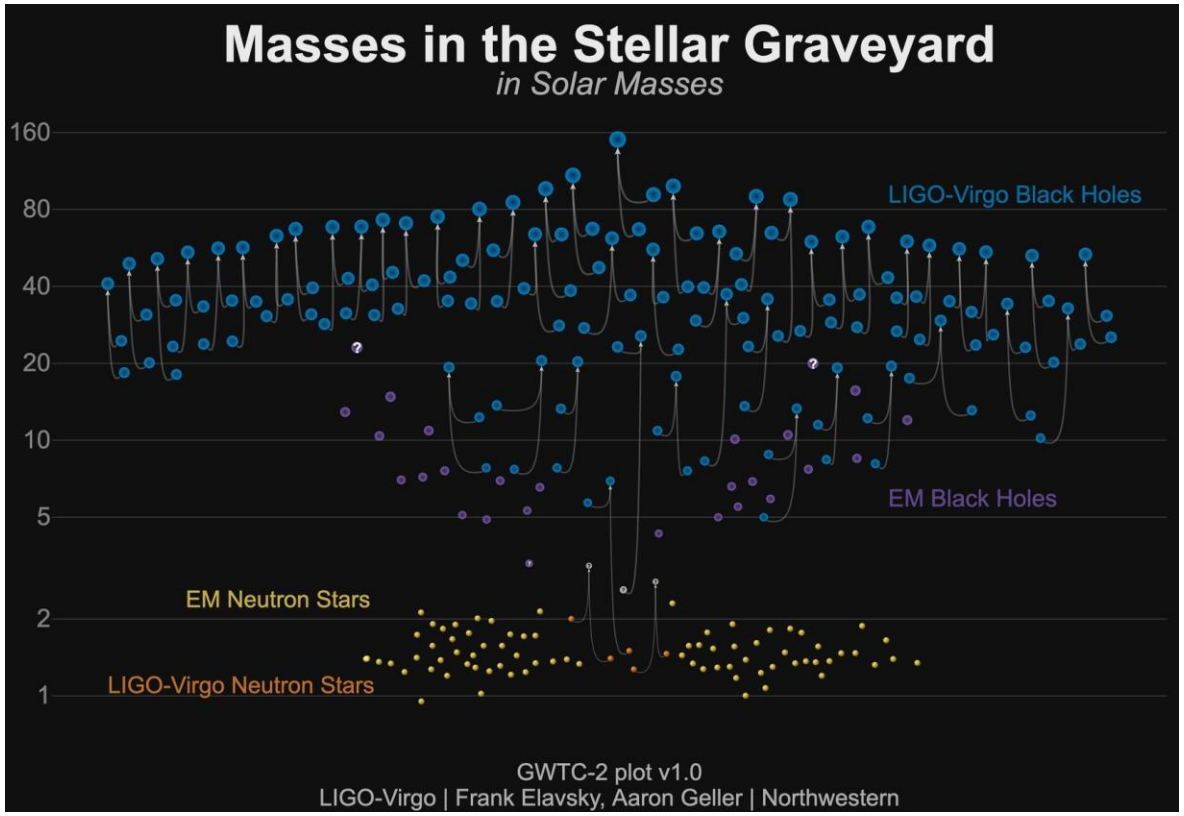

Paper Król et al. based on this analysis was recently submitted

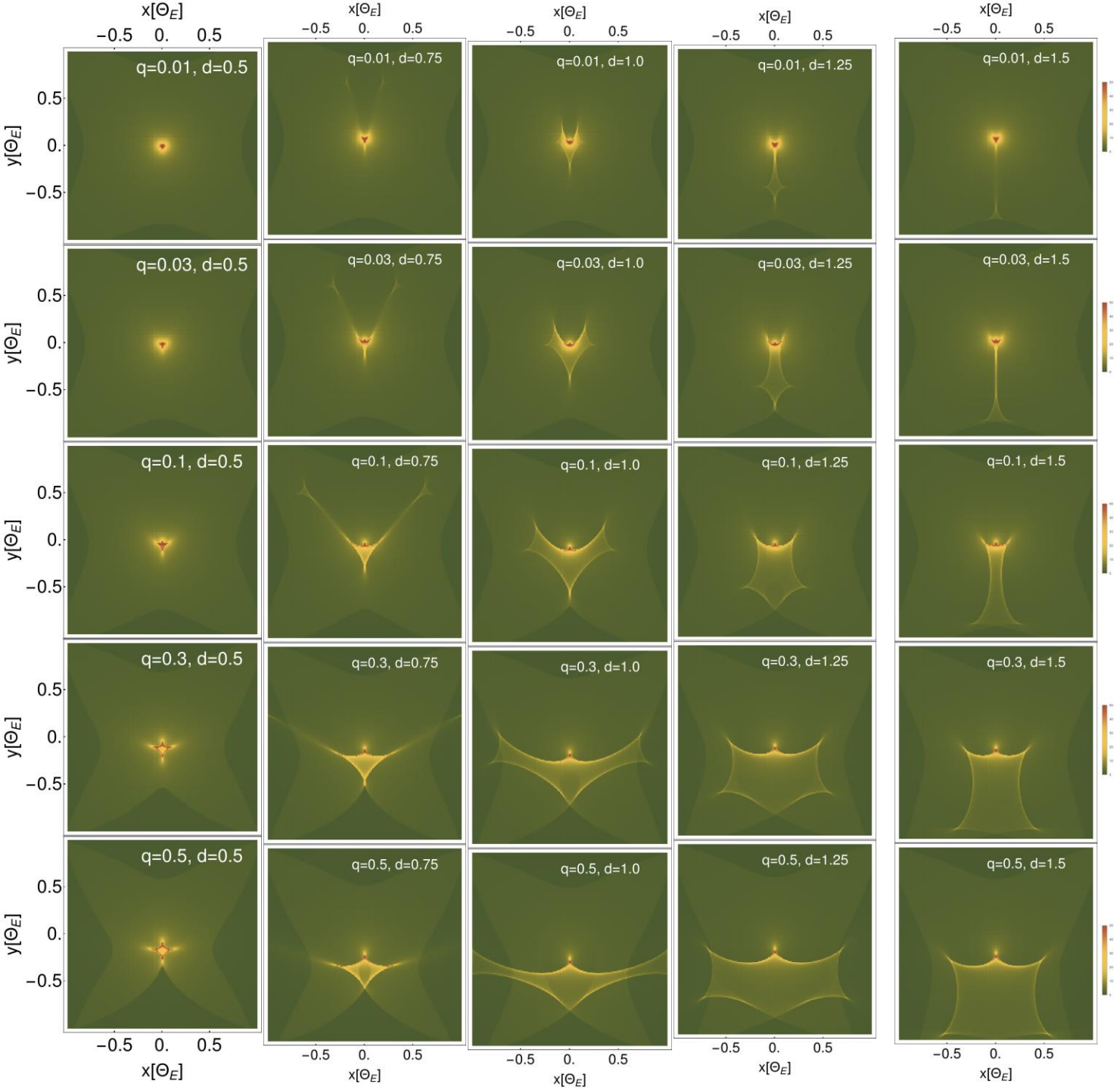

- For small separations (d), magnification occurs predominantly in a compact area surrounding the centre of mass of a binary lens.
- If, in addition, the mass ratio is < 0.01 magnification pattern resembles point-mass lens
- As mass ratio grows, the area of magnification is also enlarged, creating various shapes which exact appearance depends on the separation parameter

Fitting procedure

After initial exploration of the (q,d) parameter space through inverse ray shooting, we used MuLens Model (Poleski & Yee, 2019) to find the lens model that may fit all events.

Parameter	Name in MulensModel	Unit	Description
t_0	t_0		The time of the closest approach between the source and the lens.
u_0	u_0		The impact parameter between the source and the lens center of mass.
t_E	t_E	d	The Einstein crossing time.
ρ	rho		The radius of the source as a fraction of the Einstein ring.
s	s		The projected separation between the lens primary and its companion as a fraction of the Einstein ring radius.
q	q		The mass ratio between the lens companion and the lens primary $q \equiv m_2/m_1$.
α	alpha	deg.	The angle between the source trajectory and the binary axis.

Seven parameters is needed to describe lensing event. Three of them should be the same for all of the events (q, s, rho). Four describe the source trajectory on the lens plane – they will be different for each event

It was impossible to fit all of the parameters at the same time. So we first found the lens (q,s) which may fit all the events. Then we froze their values.

The fit was performed for each selected event separately. Since the number of the free parameter was still too large, in each fit, we selected a set of different values of tE, and fit the remaining trajectory parameters t0, u0 , and α.
The final model was chosen based on the χ2 statistic .